Schlenk-type Equilibria of Grignard-analogous Arylberyllium Complexes: Steric Effects

Christoph Helling[a,*] *and Cameron Jones*[a,*]

[a]School of Chemistry, Monash University, PO Box 23, Melbourne, VIC, 3800, Australia; E-mail: christoph.helling@monash.edu, cameron.jones@monash.edu

Abstract: The presence of complex Schlenk equilibria is a central property of synthetically invaluable Grignard reagents substantially affecting their reactivity and selectivity in chemical transformations. In this work, we systematically studied the steric effects of aryl substituents on the Schlenk-type equilibria of their lighter congeners, arylberyllium bromides. Combination of diarylberyllium complexes $Ar_2Be(OEt_2)$ (**1Ar**, Ar = Tip, Tcpp; Tip = 2,4,6-*i*$Pr_3C_6H_3$, Tcpp = 2,4,6-$Cyp_3C_6H_3$, Cyp = *c*-C_5H_9), containing sterically demanding aryl groups, and $BeBr_2(OEt_2)_2$ (**2**) affords the Grignard-analogous arylberyllium bromides $ArBeBr(OEt_2)$ (**3Ar**, Ar = Tip, Tcpp). In contrast, $Mes_2Be(OEt_2)$ (**1Mes**, Mes = 2,4,6-$Me_3C_6H_3$) and **2** exist in a temperature-dependent equilibrium with $MesBeBr(OEt_2)$ (**3Mes**) and free OEt_2. $Ph_2Be(OEt_2)$ (**1Ph**) reacts with **2** to afford dimeric $[PhBeBr(OEt_2)]_2$ (**[3Ph]$_2$**). Moreover, the influence of replacing the OEt_2 donor by an N-heterocyclic carbene, IPr_2Me_2 (IPr_2Me_2 = C(*i*PrNCMe)$_2$), on the redistribution reactions was investigated. The solution- and solid-state structures of the diarylberyllium and arylberyllium bromide complexes were comprehensively characterized using multinuclear (^{1}H, ^{9}Be, ^{13}C) NMR spectroscopic methods and single-crystal X-ray diffraction, while DFT calculations were employed to support the experimental findings.

Introduction

Since their discovery in 1900,[1] Grignard reagents of the general type $RMgX(L)_n$ (R = organyl; X = halide; L = neutral donor) developed into one of the most widely used organometallic reagents in synthetic chemistry for the construction of C−C bonds due to their straightforward preparation and reactivity, and broad applications.[2] In solution, Grignard reagents exist in complex redistribution equilibria, known as Schlenk equilibria,[3] comprising various species including $R_2Mg(L)_n$, $MgX_2(L)_n$, and dimeric as well as oligomeric species (Scheme 1). The relative abundance of each depends on the nature of the substituents R and X as well as experimental conditions such as solvent and temperature.[4]

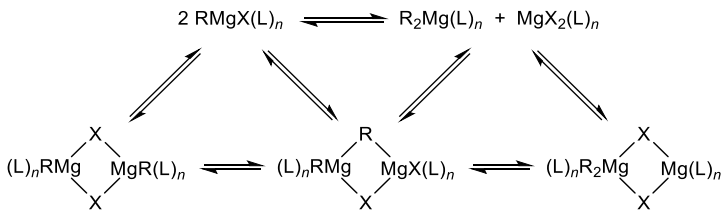

Scheme 1. Simplified Schlenk equilibrium (oligomeric species neglected).[5]

During the past decades, research also focused on the syntheses and reactivity of heavier Grignard reagents to provide alternatives with potential complementary reactivity to classical Grignard reagents,[5] whereas studies on the lighter congeners[6] have been widely neglected due to the high toxicity of beryllium and its compounds.[7] In an early report, Dessy studied the Be exchange between Ph_2Be and radiolabeled $BeBr_2$ in diethyl ether solution, with this author's analysis being that no PhBeBr (or solvates thereof) is formed in this mixture.[8] A reinvestigation by Ashby and co-workers, however, indicated that R_2Be (R = Me, Et, Ph) and BeX_2 (X = Cl, Br) redistribute rapidly in diethyl ether to form RBeX, according to selective precipitation, molecular association, and low-temperature ^{1}H NMR spectroscopic (for R = Me only) studies.[9] In a more recent report, Hanusa and co-workers observed a mixture of $R_2Be(OEt_2)$, $BeCl_2(OEt_2)_2$ and a third species, tentatively assigned to $RBeCl(OEt_2)_2$ (R = 1,3-$(Me_3Si)_2C_3H_3$), by ^{9}Be NMR spectroscopy resulting from the 1:1 reaction of $BeCl_2(OEt_2)_2$ and KR in diethyl ether. The authors considered this to be the result of a Schlenk-type equilibrium.[10] However, no evidence was provided that the observed species actually are in equilibrium, while the effect of the various coordination modes of the employed allyl substituent on a potential redistribution and the exact nature of the allylberyllium chloride are ambiguous. Moreover, $(C_5H_5)_2Be$ was found to react with BeX_2 (X = Cl, Br, I) in the absence of solvent to give $(C_5H_5)BeX$,[11] which is likely driven by change of the C_5H_5 coordination mode from η^1 to η^5. In contrast, the formation of the homoleptic β-diketiminate complex [{HC(MeCNPh)$_2$}$_2$Be] was observed upon prolonged storage of a solution of [HC(MeCNPh)$_2$]BeBr(OEt$_2$).[12] Evidently, Schlenk-type redistribution reactions of organoberyllium complexes are not yet understood, which is why we became interested in systematically investigating the redistribution reactions of diarylberyllium complexes, $Ar_2Be(OEt_2)$ (**1Ar**), with $BeBr_2(OEt_2)_2$ (**2**), and their dependence on the steric demand of the aryl substituents under comparable conditions.

Results and Discussion

For this investigation, we chose aryl substituents since they typically adopt only one coordination mode (σ), while still enabling coordination in bridging positions (μ), which might be an important feature for facilitating redistribution reactions of alkaline earth metal organyls (*cf.* Scheme 1). $BeBr_2(OEt_2)_2$ (**2**) was selected for its good solubility in aromatic solvents, while providing a diethyl ether-rich environment

precluding the impact of potential equilibria by precipitation. Moreover, beryllium bromides were discussed as most suitable starting materials for beryllium chemistry.[13] At the outset of our study, we evaluated the steric demand of potential aryl substituents by calculation of their buried volumes V_{Bur} (Table S1).[14] Based on these calculations, we included the aryls Ph, Mes (Mes = 2,4,6-$Me_3C_6H_2$), Tip (Tip = 2,4,6-*i*$Pr_3C_6H_2$), Tcpp (Tcpp = 2,4,6-$Cyp_3C_6H_2$; Cyp = *c*-C_5H_9), Tchp (Tchp = 2,4,6-$Cy_3C_6H_2$; Cy = *c*-C_6H_{11}), and Mes* (Mes* = 2,4,6-*t*$Bu_3C_6H_2$) in the experimental investigation, covering buried volumes from 26.0% to 46.7% and 15.8% to 34.6% at 3.5 Å and 5 Å sphere radius, respectively.

Recently, Buchner and co-workers reinvestigated the synthesis, properties, and reactivity of $[Ph_2Be]_3$ including determination of its solid-state structure and NMR spectroscopic characterization of the diethyl ether adduct $Ph_2Be(OEt_2)$ (**1Ph**).[14] Their synthesis involves the reaction of Be metal with $HgPh_2$ in benzene at 140 °C, whereas in their hands salt metathesis starting from $BeCl_2(OEt_2)_2$ failed to give $[Ph_2Be]_3$ or **1Ph**.[14a] In our hands, the reaction of **2** with two equivalents of PhLi in toluene gave straightforward access to $[Ph_2Be]_3$ in high yield (82%) after crystallization from diethyl ether and removal of the coordinated diethyl ether by heating under vacuum. The synthesis and solid-state structure of $Mes_2Be(OEt_2)$ (**1Mes**) were already reported by Power and co-workers, but the reported NMR data were inconsistent and incomplete.[15] We synthesized **1Mes** by a slightly modified procedure and collected consistent NMR data. Compounds **1Tip**, **1Tcpp**, and **1Tchp** were synthesized by reactions of two equivalents of the corresponding aryllithium salts with **2** in toluene and isolated after work-up as colorless crystalline solids in good yields (Scheme 2). In contrast, the reaction of two equivalents of Mes*Li with **2** only resulted in an intractable oil from which no pure compound could be isolated.

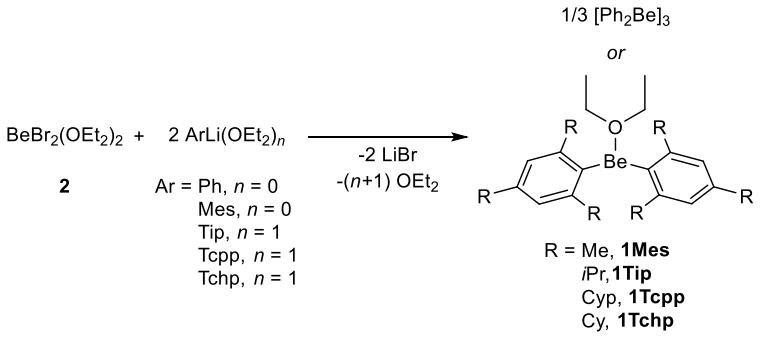

Scheme 2. Synthesis of diarylberyllium complexes **1Ar**.

Diarylberyllium complexes **1Ar** (Ar = Mes, Tip, Tcpp, Tchp) are thermally stable but highly air- and moisture-sensitive solids, which are typically soluble in aromatic solvents, except for **1Tchp**, which is practically insoluble in non-coordinating solvents once crystallized. Their ^{1}H and $^{13}C\{^{1}H\}$ NMR spectra feature the expected resonances for the corresponding aryl substituents as well as a coordinated diethyl ether. All compounds retain their coordinated diethyl ether even after prolonged placement under vacuum, which contrasts with **1Ph**. The ^{9}Be NMR spectra feature broad resonances (**1Mes** 20.2

ppm, $\omega_{1/2}$ = 275 Hz; **1Tip** 18.7 ppm, $\omega_{1/2}$ = 490 Hz; **1Tcpp** 18.2 ppm, $\omega_{1/2}$ ≈ 667 Hz; **1Tchp** 18.2 ppm, $\omega_{1/2}$ ≈ 650 Hz), comparable to that of **1Ph** (18.6 ppm, $\omega_{1/2}$ = 154 Hz)[14a] and in accordance with three-coordinate Be centers.[16] The ^{9}Be resonances are particularly broad for the complexes containing sterically more demanding aryl substituents. The solid-state structures of **1Tip**, **1Tcpp**, and **1Tchp** (Figures 1, S82) were determined by single-crystal X-ray diffraction analysis, confirming the formation of diarylberyllium-diethyl ether adducts. These extend the surprisingly small number of structurally characterized arylberyllium complexes. Suitable crystals were obtained from solutions in *n*-hexane (**1Tip**, **1Tcpp**) or diethyl ether (**1Tchp**).

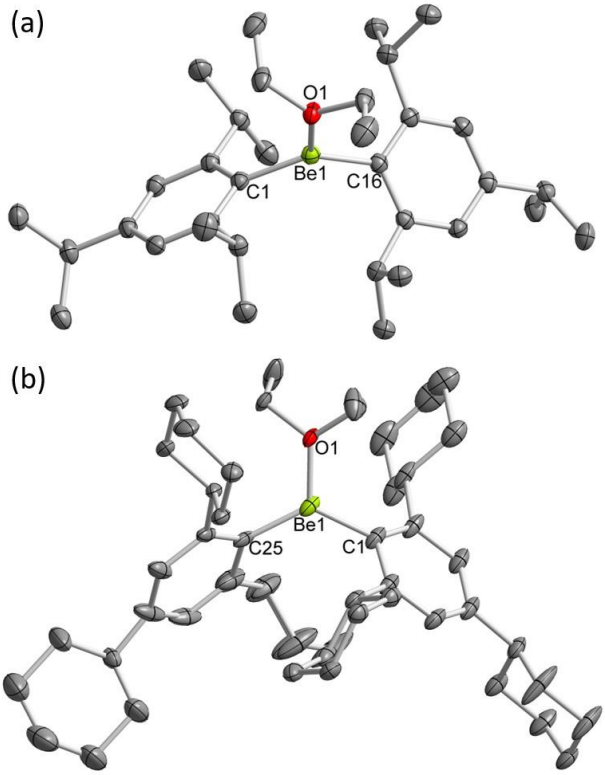

Figure 1. Molecular structures of (a) **1Tip** and (b) **1Tchp** in the solid-state. Hydrogen atoms and the minor component of the disordered Cy group in **1Tchp** were omitted for clarity. Displacement ellipsoids are drawn at 50% probability level.

The molecular structures feature three-coordinate planar geometries at the Be centers with Be–C (**1Tip** 1.7690(17) Å, 1.7678(17) Å; **1Tcpp** 1.753(3) Å, 1.759(3) Å; **1Tchp** 1.759(3) Å, 1.760(3) Å) and Be–O (**1Tip** 1.6574(17) Å; **1Tcpp** 1.665(3) Å; **1Tchp** 1.649(2) Å) bond lengths comparable to those of **1Mes** (Be–C 1.739(3) Å; Be–O 1.638(5) Å)[15] and $Ph_2Be(OnBu_2)$ (Be–C 1.734(2) Å, 1.745(2) Å; Be–O 1.647(2) Å).[17] The C–Be–C bond angles of **1Tip** (133.18(9)°) and **1Tcpp** (134.63(18)°) are wider than those of **1Mes** (127.6(3)°) and $Ph_2Be(OnBu_2)$ (127.79(13)°), as expected due to the increased steric demand of the aryl substituents. Interestingly, the corresponding angle of even more sterically congested **1Tchp** (127.68(15)°) is virtually identical to those of **1Mes** and $Ph_2Be(OnBu_2)$, presumably due to London dispersion interactions between the Cy groups.[18]

With **1Ar** in hand, we targeted an investigation of redistribution reactions with **2**. Accordingly, the corresponding diarylberyllium **1Ar** was combined with **2** in C_6D_6 and the reaction progress was monitored by ^{1}H and ^{9}Be NMR spectroscopy. Combination of *in situ* generated **1Ph** and **2** immediately resulted in a pronounced shift of the ^{9}Be NMR resonance from 18.6 ppm ($\omega_{1/2}$ = 154 Hz, **1Ph**) to 7.8 ppm ($\omega_{1/2}$ = 95 Hz) with concomitant sharpening of the resonance indicating the formation of a new, tetracoordinate Be species (Figure S55),[16] while less pronounced yet significant shifts of the ^{1}H resonances were observed (Figure S54). In order to probe a potential influence of the limited amount of diethyl ether present, an excess of diethyl ether was added, which did not cause a significant shift of the ^{1}H and ^{9}Be NMR resonances. Moreover, essentially the same NMR spectra were obtained from combination of three equivalents of **2** and $[Ph_2Be]_3$. Repetition of the experiment on a preparative scale in diethyl ether and subsequent crystallization from dichloromethane/*n*-hexane afforded colorless crystals in moderate yield, which were identified as dimeric $[PhBeBr(OEt_2)]_2$ (**[3Ph]$_2$**) by single-crystal X-ray diffraction (Figure 2, Scheme 3a).

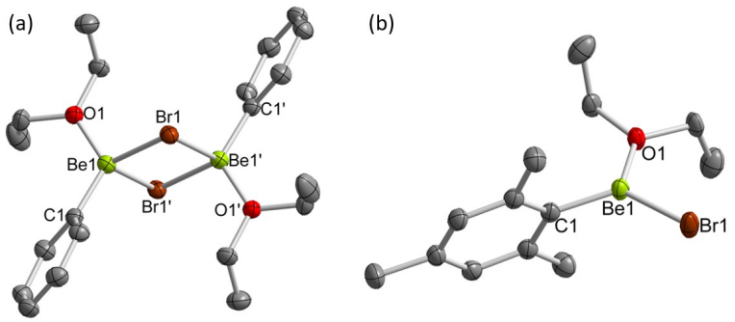

Figure 2. Molecular structure of (a) **[3Ph]$_2$** and (b) **3Mes** in the solid-state. Hydrogen atoms and the second independent molecule of **3Mes** were omitted for clarity. Displacement ellipsoids are drawn at 50% probability level.

The molecular structure of the centrosymmetric dimer **[3Ph]$_2$** consists of two $PhBeBr(OEt_2)$ moieties bridged *via* the bromide substituents resulting in distorted tetrahedrally coordinated Be centers with Br–Be–Br' and C–Be–O bond angles of 98.21(10)° and 119.83(18)°, respectively. The Be–Br (2.243(3) Å) and Be–Br' (2.339(3) Å) bond lengths are slightly longer than those of donor-stabilized $BeBr_2$ dimers, $[(L)BeBr_2]_2$ (L = SMe_2 2.0809(14), 2.212(3) Å;[19] NEt_3 2.108(2)–2.281(2) Å;[20] DMF 2.110(3)–2.292(2) Å[13]), while the Be–C (1.745(3) Å) and Be–O (1.639(3) Å) bond lengths are in agreement with those of **1Ar** (Ar = Mes, Tip, Tcpp, Tchp) and $Ph_2Be(OnBu_2)$.[15,17]

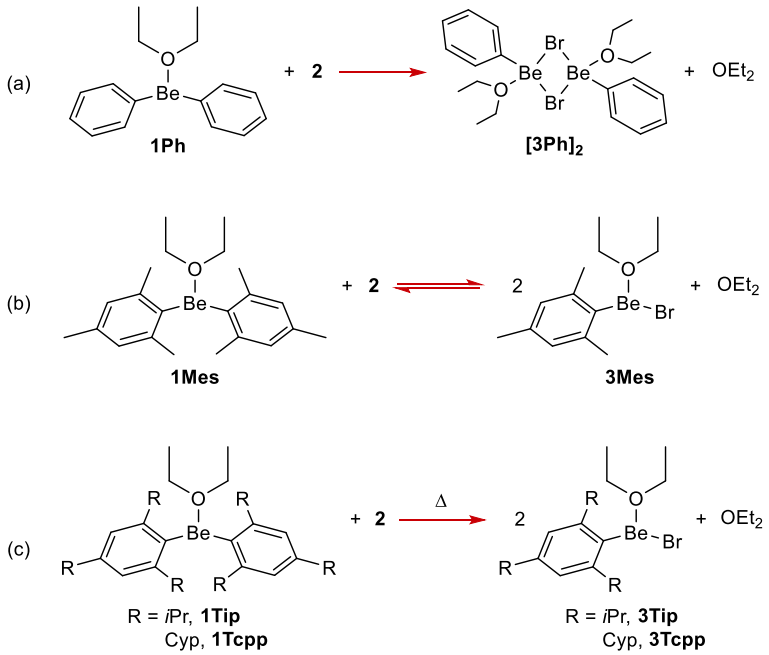

Scheme 3. Reactivity of **1Ar** with **2**.

The multinuclear NMR spectra of isolated crystals of **[3Ph]$_2$** are essentially identical to those of the reaction mixtures featuring the expected resonances for the Ph substituent and OEt_2 donor in a 1:1 ratio. As mentioned, the ^{9}Be NMR resonance at 7.8 ppm suggests that the Be centers are tetracoordinate indicating that the dimeric structure is retained in solution. This is supported by DFT calculations, which predict a ^{9}Be NMR shift for **[3Ph]$_2$** of 6.5 ppm close to the experimentally observed shift, whereas that for the corresponding monomer was predicted to be 13.8 ppm. Moreover, the estimated molecular weight of 404 g mol^{-1} from ^{1}H DOSY NMR measurements (Figure S53, Table S2)[21] corresponds to that of dimeric **[3Ph]$_2$** (480.29 g mol^{-1}), further supporting the presence of dimeric **[3Ph]$_2$** in benzene solution. A variable-temperature ^{1}H and ^{9}Be NMR spectroscopic study (Figures S56–S59) showed no indications for the presence of a temperature-dependent Schlenk-type equilibrium since neither $[Ph_2Be]_3$ nor **1Ph** were observed in these spectra. The conclusions from the experimental observations are supported by DFT calculations, which showed that reactions of $[Ph_2Be]_3$ and **1Ph** with **2** are both exothermic and exergonic ($[Ph_2Be]_3$ ΔH = -10.0 kcal mol^{-1}, ΔG^{298} = -7.5 kcal mol^{-1}; **1Ph** ΔH = -3.9 kcal mol^{-1}, ΔG^{298} = -3.5 kcal mol^{-1}), whereas dissociation of **[3Ph]$_2$** into **3Ph** was calculated to be both endothermic and endergonic (ΔH = 18.3 kcal mol^{-1}, ΔG^{298} = 3.6 kcal mol^{-1}). Although these results indicate that **[3Ph]$_2$** likely is the major species in benzene solution, fast exchange processes in solution even at low temperatures resulting in averaged NMR signals. Also, exclusive crystallization of **[3Ph]$_2$** from an equilibrium mixture could obscure the actual presence of other species, *i.e.*, **2** and $[Ph_2Be]_3$ or **1Ph** in solution. Given the low solubility of $[Ph_2Be]_3$, the latter is unlikely.

The ^{1}H and ^{9}Be NMR spectra of the reaction mixture of equimolar amounts of **1Mes** and **2** immediately showed partial formation of a new three-coordinate Be species containing Mes substituents as

deduced from the presence of corresponding ^{1}H resonances as well as a new ^{9}Be resonance (15.7 ppm, $\omega_{1/2}$ = 94 Hz) in the NMR spectra (Figures S60 and S61). No further conversion was observed upon storage at ambient temperature or heating to 100 °C overnight. ^{1}H DOSY NMR measurements (Figure S62, Table S3) showed the presence of two Mes containing species with estimated molecular weights[21] of 419 g mol^{-1} and 294 g mol^{-1} assigned to **1Mes** and MesBeBr(OEt$_2$) (**3Mes**), respectively. A variable-temperature NMR spectroscopic study (Figures S63, S64) revealed the presence of a temperature-dependent Schlenk-type equilibrium according to Scheme 3b with **3Mes** and free OEt$_2$ being the dominant species at elevated temperatures and **1Mes** and **2** being favored at low temperatures. To the best of our knowledge, this is the first time such an equilibrium was directly observed in organoberyllium chemistry. Interestingly, below -20 °C the equilibrium is frozen yielding no further reconversion of the starting materials, which indicates a considerable activation barrier for the process. A Van 't Hoff analysis (Figures 3b, S67, Table S4) generated from ^{1}H NMR data in the temperature range 27–72 °C (Figures 3a, S65, S66) yielded ΔH = 15.78 kcal mol^{-1} and ΔS = 0.0464 cal mol^{-1} K^{-1} resulting in ΔG^{298} = 1.95 kcal mol^{-1} (Tables S5, S6), revealing an endothermic, entropy driven redistribution reaction.

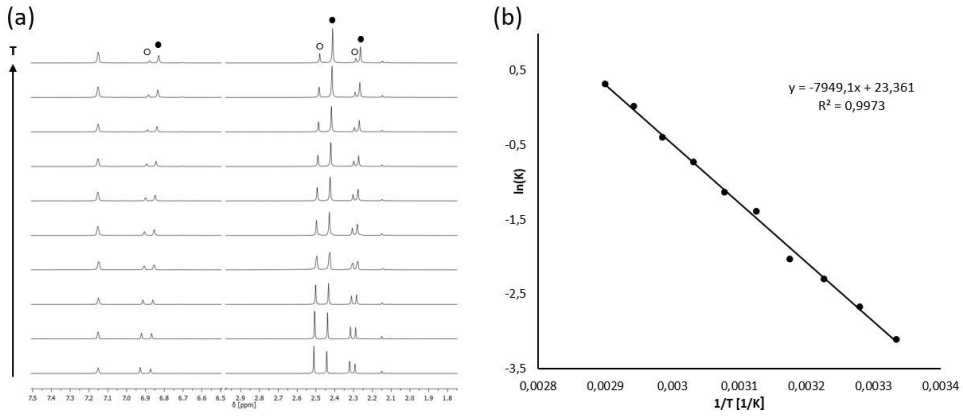

Figure 3. (a) Variable-temperature ^{1}H NMR spectra of an equimolar mixture of **1Mes** and **2** and (b) corresponding Van 't Hoff plot (○ = **1Mes**, ● = **3Mes**).

The experimentally obtained values are in reasonable agreement with the calculated values by means of DFT (ΔH = 12.9 kcal mol^{-1}, ΔG^{298} = -3.4 kcal mol^{-1}). Addition of an excess of diethyl ether to the reaction mixture results in a shift of the equilibrium towards the starting materials, whereas removal of volatiles shifted the equilibrium towards formation of **3Mes** according to Le Chatelier's principle (Figures S68, S69). Eventually, **3Mes** was isolated in moderate yield by repeated addition and removal of benzene with subsequent crystallization from toluene/*n*-hexane, then fully characterized. The multinuclear NMR spectra of **3Mes** are consistent with the proposed structure. A single-crystal X-ray diffraction study confirmed the monomeric nature of **3Mes** with three-coordinate planar Be centers (Figure 2), which is in contrast to the observed association of **[3Ph]$_2$**. This is presumably caused by the

increased steric demand of Mes compared to Ph rendering dimer formation unfavorable and demonstrates the delicate influence of steric effects on the structures and solution processes of arylberyllium complexes. Support for this was gained through DFT calculations, according to which the dimerization of **3Ph** is exergonic (ΔG^{298} = -3.6 kcal mol^{-1}), whereas that of **3Mes** is endergonic (ΔG^{298} = 11.73 kcal mol^{-1}). The crystal structure of **3Mes** exhibits two independent yet virtually identical molecules in the asymmetric unit, which are loosely associated by *p*-C*H*$_3$···arene contacts. The Be–C (1.725(3), 1.725(4) Å), Be–Br (2.073(3), 2.082(4) Å) and Be–O (1.595(3), 1.592(3) Å) bond lengths are comparable to those of [2,6-(2,4,6-$R_3C_6H_2$)$_2$C$_6$H$_3$]BeBr(OEt$_2$) (R = H, Be–C 1.724(3) Å, Be–Br 2.087(3) Å, Be–O 1.593(3) Å;[12] Me, Be–C 1.749(7) Å, Be–Br 2.071(6) Å, Be–O 1.612(7) Å [22]). The terminal Be–Br distances in **3Mes** are shorter than those of the Be–Br–Be bridges in **[3Ph]$_2$**, which was also observed in dimeric BeBr$_2$ adducts.[13,19,20]

Treatment of **1Tip** and **1Tcpp** with one equivalent of **2** at ambient temperature, respectively, immediately resulted in partial conversion to new species containing the corresponding ligands, as deduced from the ^{1}H NMR spectra of the reaction mixtures (Figures S70, S71, S74, S75). However, full conversion to the new products was only obtained after heating the reaction mixtures to 100 °C overnight. Independent synthesis of the arylberyllium bromides TipBeBr(OEt$_2$) (**3Tip**) and TcppBeBr(OEt$_2$) (**3Tcpp**) *via* salt metathesis reactions of equimolar amounts of **2** and the corresponding aryllithium salts, TipLi(OEt$_2$) and TcppLi(OEt$_2$), respectively (Scheme 4), allowed for the identification of the new species in the redistribution reactions as **3Tip** and **3Tcpp** by comparison of the ^{1}H and ^{9}Be NMR spectroscopic data. No reconversion to **2** and **1Tip** and **1Tcpp**, respectively, was observed upon storage at ambient temperature. Moreover, addition of an excess of diethyl ether before or after the thermal treatment of **1Tip** and **2** to induce ligand redistribution did not affect the outcome (Figures S72, S73). The fact that **3Tcpp** was recovered in good yield after recrystallization from diethyl ether further demonstrates the irreversibility of the redistribution for aryberyllium bromides containing sterically demanding aryl substituents. DFT calculations predict endothermic and only slightly exergonic redistribution processes (Ar = Tip, ΔH = 15.2 kcal mol^{-1}, ΔG^{298} = -0.3 kcal mol^{-1}; Tcpp, ΔH = 13.9 kcal mol^{-1}, ΔG^{298} = -4.7 kcal mol^{-1}), indicating that there is a considerable activation barrier for the reverse process in case of **3Tip**.

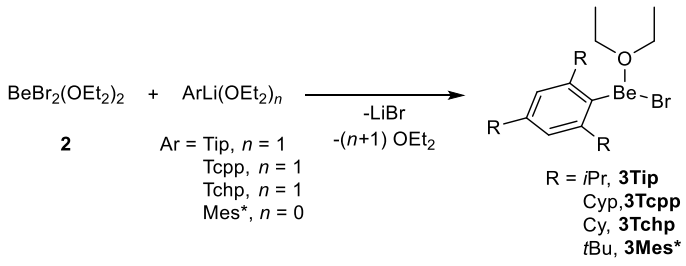

Scheme 4. Synthesis of arylberyllium bromides **3Ar**.

The redistribution reaction of **1Tchp** with **2** could not be studied under analogous conditions to those of **1Tip** and **1Tcpp** due to the insolubility of **1Tchp** in benzene, which is why THF-d_8 was employed. No conversion was observed at ambient temperature, whereas heating to 100 °C overnight resulted in unselective conversion to free arene and several tetracoordinate Be species as observed in the ^{1}H and ^{9}Be NMR spectra (Figure S76, S77). This could result from decomposition of $BeBr_2(THF)_2$ at elevated temperatures as observed for $BeI_2(THF)_2$.[23] Nevertheless, arylberyllium bromides TchpBeBr(OEt_2) (**3Tchp**) and Mes*BeBr(OEt_2) (**3Mes***) were synthesized for the sake of completeness by salt metathesis reactions analogous to **3Tip** and **3Tcpp** and obtained in moderate yields after crystallization (Scheme 4).

3Ar (Ar = Tip, Tcpp, Tchp, Mes*) show the expected features of the aryl substituents and coordinated diethyl ether in their ^{1}H and ^{13}C NMR spectra, which integrated in a 1:1 ratio. The ^{9}Be NMR spectra of **3Ar** (Ar = Tip 16.0 ppm, $\omega_{1/2}$ = 176 Hz; Tcpp 16.1 ppm, $\omega_{1/2}$ = 296 Hz; Tchp 16.3 ppm, $\omega_{1/2}$ = 398 Hz; Mes* 13.4 ppm, $\omega_{1/2}$ = 183 Hz) exhibit broad resonances consistent with the three-coordinate nature of the Be centers and which are comparable to that of **3Mes** (15.7 ppm, $\omega_{1/2}$ = 94 Hz). The solid-state structures of **3Ar** (Ar = Tip, Tcpp, Tchp, Mes*; Figures 4, S83, S84) were determined by single-crystal X-ray diffraction analysis showing monomeric arylberyllium bromides with virtually identical Be–C (Ar = Tip 1.724(2) Å, Tcpp 1.725(4) Å, Tchp 1.722(2) Å, Mes* 1.741(6) Å), Be–Br (Ar = Tip 2.0754(18) Å, Tcpp 2.084(3) Å, Tchp 2.0755(19) Å, Mes* 2.106(5) Å), and Be–O (Ar = Tip 1.602(2) Å, Tcpp 1.602(4) Å, Tchp 1.599(2) Å, Mes* 1.630(5) Å) bond distances, which are in good agreement with those of **3Mes** and [2,6-(2,4,6-$R_3C_6H_2)_2C_6H_3$]BeBr(OEt_2) (R = H, Me).[12,22] The C–Be–Br bond angles (Ar = Mes 125.80(16)°, 125.61(18)°, Tip 124.28(11)°, Tcpp 124.92(19)°, Tchp 124.25(11)°, Mes* 123.8(3)°) are smaller than the C–Be–C bond angles of diarylberyllium complexes **1Ar**.

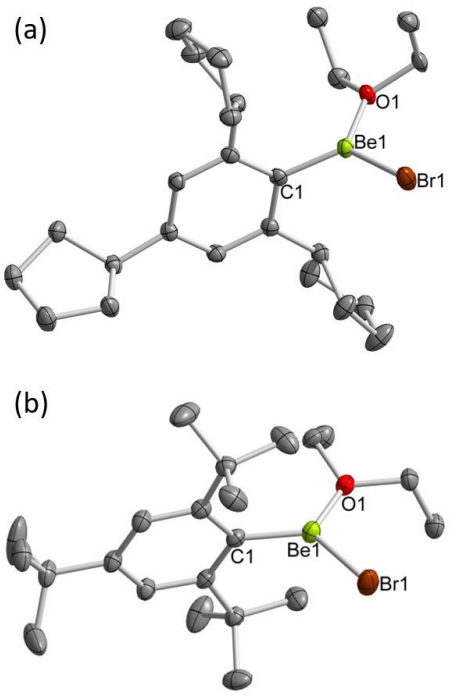

Figure 4. Molecular structure of (a) **3Tcpp** and (b) **3Mes*** in the solid-state. Hydrogen atoms were omitted for clarity. Displacement ellipsoids are drawn at 50% probability level.

To evaluate the effect of potentially dissociating diethyl ether donors, redistribution reactions of more strongly bound carbene-coordinated Be complexes, (IPr_2Me_2)$BeAr_2$ (Ar = Ph **4Ph**,[17] Mes **4Mes**; IPr_2Me_2 = C(*i*PrNCMe)$_2$) and (IPr_2Me_2)$BeBr_2$ (**5**),[24] were investigated. IPr_2Me_2 was chosen since it is the least sterically demanding carbene (V_{Bur} 31.7%, 42.1% for the conformers with C*H*$(CH_3)_2$ oriented towards and away from the Be center, respectively) of which 1:1 complexes with $BeBr_2$[24,25] and $BePh_2$[15b,17] are known. **4Mes** was synthesized in high yield by straightforward ligand exchange reaction of **1Mes** and IPr_2Me_2. Its ^{1}H and ^{13}C{^{1}H} NMR spectra exhibit the expected resonances for the carbene and the Mes substituents, while the ^{9}Be NMR spectrum features a broad resonance at 23.0 ppm ($\omega_{1/2}$ = 424 Hz), which is similar to that of reported **4Ph** (21.1 ppm, $\omega_{1/2}$ = 464 Hz).[17] The molecular structure of **4Mes** as determined by single-crystal X-ray diffraction (Figure S85) shows a three-coordinate planar Be center with similar Be–C_{Aryl} (1.7676(14) Å) and Be–$C_{Carbene}$ (1.803(2) Å) bond lengths that correspond to those of **4Ph** (Be–C_{Aryl} 1.757(4), 1.745(4) Å; Be–$C_{Carbene}$ 1.807(4) Å).[17] Combination of **4Ph** with **5** immediately resulted in formation of a new species as observed in the ^{1}H and ^{9}Be NMR spectra of the reaction mixture (Scheme 5), which was identified as (IPr_2Me_2)PhBeBr (**6Ph**) by comparing the NMR spectroscopic data with an authentic, isolated sample of **6Ph** independently synthesized by addition of IPr_2Me_2 to a solution of **[3Ph]$_2$**. Similarly, **4Mes** reacts with **5** at 100 °C to give (IPr_2Me_2)MesBeBr (**6Mes**) albeit with lower selectivity due to side reactions such as formation of (IPr_2Me_2)$_2BeBr_2$ (Scheme 5). **6Mes** was independently synthesized by addition of IPr_2Me_2 to a mixture of **1Mes** and **2** at 80 °C.

These reactions demonstrate that Schlenk-type redistribution reactions of arylberyllium complexes also proceed when diethyl ether is replaced by stronger donors such as carbenes.

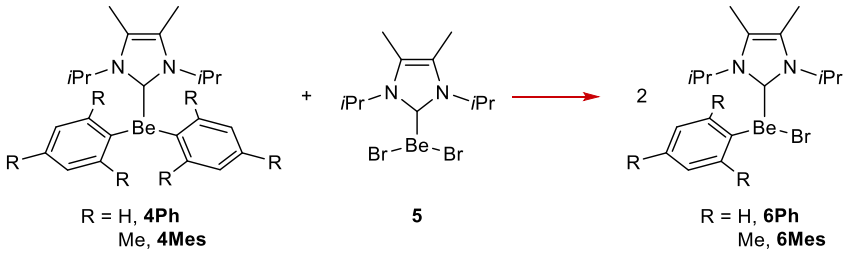

Scheme 5. Reactivity of **4Ar** with **5**.

Compounds **6Ph** and **6Mes** were isolated as colorless crystalline solids in moderate yields. Their ^{1}H and ^{13}C{^{1}H} NMR spectra feature the expected resonances for the carbene ligand and aryl substituent, which integrated in a 1:1 ratio, while the ^{9}Be NMR spectra exhibit resonances at 18.5 ppm ($\omega_{1/2}$ = 223 Hz, **6Ph**) and 19.1 ppm ($\omega_{1/2}$ = 227 Hz, **6Mes**), reflecting the three-coordinate environment at the Be centers. The ^{9}Be resonance also compares well to that of [(HCNDip)$_2$C]PhBeCl (19.0 ppm, $\omega_{1/2}$ = 277 Hz; Dip = 2,6-*i*Pr$_2$C$_6$H$_3$).[15c] The solid-state structures of **6Ph** and **6Mes** (Figure 5) derived from single-crystal X-ray diffraction show monomeric carbene-supported arylberyllium bromides with Be–C$_{Aryl}$ (**6Ph** 1.761(8) Å, 1.738(7) Å; **6Mes** 1.739(3) Å) and Be–C$_{Carbene}$ (**6Ph** 1.773(8) Å, 1.778(7) Å; **6Mes** 1.778(3) Å) bond lengths close to those of **4Ph** and **4Mes**.

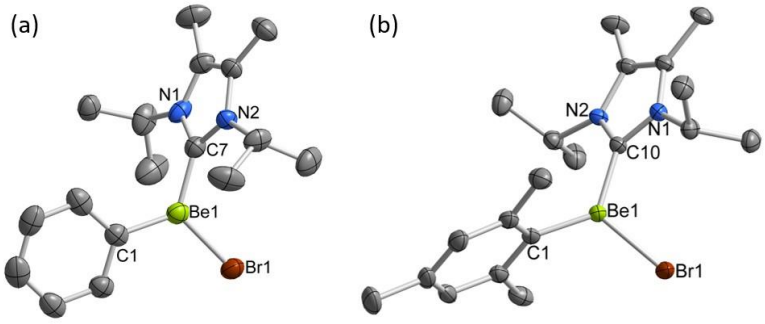

Figure 5. Molecular structure of (a) **6Ph** and (b) **6Mes** in the solid-state. Hydrogen atoms and the second independent molecule of **6Ph** were omitted for clarity. Displacement ellipsoids are drawn at 50% probability level.

The Be–Br bond lengths in **6Ph** (2.106(6), 2.119(6) Å) and **6Mes** (2.112(2) Å) are slightly longer than those in complexes **3Ar**, presumably due to the stronger electron-donating character of the carbene in comparison to diethyl ether. The molecular structures of **6Ph** and **6Mes** illustrate the consequences of the increased steric bulk of Mes compared to Ph, in that C*H*(CH$_3$)$_2$ protons are oriented away from the Be center in **6Ph**, whereas they are oriented towards the Be center in **6Mes**. Moreover, **[3Ph]$_2$** was

found to be dimeric, whereas **6Ph** is monomeric, presumably demonstrating the increased steric demand and electron-donating properties of IPr_2Me_2 compared to diethyl ether.

Conclusion

In summary, we systematically investigated Schlenk-type redistribution reactions between diarylberyllium complexes **1Ar** and beryllium bromide **2**. Accordingly, the new diarylberyllium complexes **1Tip**, **1Tcpp**, and **1Tchp** containing bulky aryl substituents were synthesized and characterized. Depending on the steric demand of the aryl substituent differing reactivity was observed. The ligand redistribution between **1Ph** and **2** is driven by dimerization of $PhBeBr(OEt_2)$ to afford **[3Ph]$_2$**. **1Mes** and **2** exist in a temperature-dependent equilibrium with **3Mes** and free OEt_2, which can be manipulated by addition or removal of diethyl ether. The thermodynamic parameters for this equilibrium were extracted from a Van 't Hoff analysis revealing the redistribution to be endothermic and entropy driven. In case of **3Tip** and **3Tcpp**, complete ligand redistribution occurs at elevated temperatures and this exhibits no reversibility. The corresponding arylberyllium bromides **[3Ph]$_2$**, **3Mes**, **3Tip**, and **3Tcpp** were isolated and their structures confirmed by single-crystal X-ray diffraction. Additionally, the bulky arylberyllium bromides **1Tchp** and **1Mes*** were synthesized by salt metathesis reactions. Irreversible ligand redistribution reactions were also found to occur between carbene-coordinated diarylberyllium and beryllium dibromide complexes **4Ar** and **5** to afford carbene-stabilized arylberyllium bromides **6Ph** and **6Mes**. Hence, this study revealed the delicate influence of the aryl substituent's steric demand on redistribution processes of organoberyllium complexes providing, fundamental insight for future investigations into the organometallic chemistry of beryllium.

Acknowledgements

C.H. thanks the Alexander von Humboldt foundation for a Feodor Lynen fellowship. CJ thanks the Australian Research Council for funding. Moreover, this material is based upon work supported by the Air Force Office of Scientific Research under award number FA2386-21-1-4048. Part of this research was undertaken on the MX1 beam line at the Australian Synchrotron, Victoria, Australia. The authors thank Dr. Matthew J. Evans for support with the X-ray diffraction experiments and Dr. Alasdair I. McKay for the variable-temperature and DOSY NMR measurements.

Conflict of interest

There are no conflicts to declare.

References

[1] V. C. Grignard, *Compt. Rend. Hebd. Séances Acad. Sci.* **1900**, *130*, 1322−1324.

[2] D. Seyferth, *Organometallics* **2009**, *28*, 1598−1605.

[3] W. Schlenk, W. Schlenk Jr., *Ber. Dtsch. Chem. Ges. B* **1929**, *62*, 920−924; b) W. Schlenk Jr., *Ber. Dtsch. Chem. Ges.* **1931**, *64*, 734−736.

[4] a) J. Meisenheimer, W. Schlichenmaier. *Ber. Dtsch. Chem. Ges.* **1928**, *61*, 720−729; b) D. F. Evans, M. S. Khan, *J. Chem. Soc. A* **1967**, 1643−1648; c) F. W. Walker, E. C. Ashby, *J. Am. Chem. Soc.* **1969**, *91*, 3845−3850; d) E. C. Ashby, G. Parris, F. Walker, *J. Chem. Soc. D* **1969**, 1464−1464; e) D. F. Evans, G. V. Fazakerley, *J. Chem. Soc. A* **1971**, 184−189.

[5] a) M. Westerhausen, M. Gärtner, R. Fischer, J. Langer, L. Yu, M. Reiher, *Chem. Eur. J.* **2007**, *13*, 6292−6306; b) M. Westerhausen, *Coord. Chem. Rev.* **2008**, *252*, 1516−1531; c) M. Westerhausen, A. Koch, H. Görls, S. Krieck, *Chem. Eur. J.* **2017**, *23*, 1456−1483; d) A. Koch, Q. Dufrois, M. Wirgenings, H. Görls, S. Krieck, M. Etienne, G. Pohnert, M. Westerhausen, *Chem. Eur. J.* **2018**, *24*, 16840−16850; e) P. Schüler, S. Sengupta, S. Krieck, M. Westerhausen, *Chem. Eur. J.* **2023**, *29*, e202300833.

[6] A few reports describe the synthesis of RBeX (R = alkyl; X = Cl, Br) by redistribution reactions of R_2Be and BeX_2 but their conclusions are rather speculative due to insufficient analytical evidence: a) H. Gilman, F. Schulze, *J. Am. Chem. Soc.* **1927**, *49*, 2904–2908; b) G. E. Coates, B. R. Francis, *J. Chem. Soc. A* **1971**, 1305–1308; c) N. Atam, K. Dehnicke, *Z. Anorg. Allg. Chem.* **1976**, *427*, 193–199. See also: G. E. Coates, G. L. Morgan, *Adv. Organomet. Chem.* **1971**, *9*, 195–257.

[7] a) M. R. Buchner, *Z. Naturforsch. B* **2020**, *75*, 405–412; b) M. R. Buchner, M. Müller, *ACS Chem. Health Saf.* **2023**, *30*, 36–43; c) D. Naglav, M. R. Buchner, G. Bendt, F. Kraus, S. Schulz, *Angew. Chem. Int. Ed.* **2016**, *55*, 10562–10576; d) M. R. Buchner, *Chem. Commun.* **2020**, *56*, 8895–8907.

[8] R. E. Dessy, *J. Am. Chem. Soc.* **1960**, *82*, 1580–1582.

[9] a) E. C. Ashby, J. R. Sanders, J. H. Carter, *Chem. Commun.* **1967**, 997–998; b) J. R. Sanders, E. C. Ashby, J. H. Carter, *J. Am. Chem. Soc.* **1968**, *90*, 6385–6390.

[10] a) S. C. Chmely, T. P. Hanusa, W. W. Brennessel, *Angew. Chem. Int. Ed.* **2010**, *49*, 5870–5874; b) N. C. Boyde, N. R. Rightmire, T. P. Hanusa, W. W. Brennessel, *Inorganics* **2017**, *5*, 36.

[11] D. A. Drew, G. L. Morgan, *Inorg. Chem.* **1977**, *16*, 1704–1708.

[12] A. Paparo, C. Jones, *Chem. Asian J.* **2019**, *14*, 486–490.

[13] M. Müller, M. R. Buchner, *Inorg. Chem.* **2019**, *58*, 13276-13284.

[14] L. Falivene, Z. Cao, A. Petta, L. Serra, A. Poater, R. Olivia, V. Scarano, L. Cavallo, *Nat. Chem.* **2019**, *11*, 872–879.

[15] a) M. Müller, M. R. Buchner, *Chem. Eur. J.* **2020**, *26*, 9915–9922; b) L. R. Thomas-Hargreaves, M. Müller, N. Spang, S. I. Ivlev, M. R. Buchner, *Organometallics* **2021**, *40*, 3797–3807; c) L. R. Thomas-Hargreaves, C. Berthold, W. Augustinov, M. Müller, S. I. Ivlev, M. R. Buchner, *Chem. Eur. J.* **2022**, *28*, e202200851; d) L. R. Thomas-Hargreaves, Y.-Q. Liu, Z.-H. Cui, S. Pan, M. R. Buchner, *J. Comput. Chem.* **2023**, *44*, 397–405.

[15] K. Ruhlandt-Senge, R. A. Bartlett, M. M. Olmstead, P. P. Power, *Inorg. Chem.* **1993**, *32*, 1724–1728.

[16] a) P. G. Plieger, K. D. John, T. S. Keizer, T. M. McCleskey, A. K. Burrell, R. L. Martin, *J. Am. Chem. Soc.* **2004**, *126*, 14651–14658; b) J. K. Buchanan, P. G. Plieger, *Z. Naturforsch. B* **2020**, *75*, 459–472.

[17] J. Gottfriedsen, S. Blaurock, *Organometallics* **2006**, *25*, 3784–3786.

[18] C. R. Stennett, M. Bursch, J. C. Fettinger, S. Grimme, P. P. Power, *J. Am. Chem. Soc.* **2021**, *143*, 21478–21483.

[19] M. R. Buchner, L. R. Thomas-Hargreaves, L. K. Kreuzer, N. Spang, S. I. Ivlev, *Eur. J. Inorg. Chem.* **2021**, 4990–4997.

[20] M. R. Buschner, M. Müller, N. Spang, *Dalton Trans.* **2020**, *49*, 7708–7712.

[21] a) R. Evans, Z. Deng, A. K. Rogerson, A. S. McLachlan, J. J. Richards, M. Nilsson, G. A. Morris, *Angew. Chem. Int. Ed.* **2013**, *52*, 3199–3202; b) R. Evans, G. Dal Poggetto, M. Nilsson, G. A. Morris, *Anal. Chem.* **2018**, *90*, 3987–3994.

[22] M. Niemeyer, P. P. Power, *Inorg. Chem.* **1997**, *36*, 4688–4696.

[23] D. F. Bekis, L. R. Thomas-Hargreaves, C. Berthold, S. I. Ivlev, M. R. Buchner, *Z. Naturforsch. B* **2023**, *78*, 165–173.

[24] L. R. Thomas-Hargreaves, S. Pan, S. I. Ivlev, G. Frenking, M. R. Buchner, *Inorg. Chem.* **2022**, *61*, 700–705.

[25] W. A. Herrmann, O. Runte, G. Artus, *J. Organomet. Chem.* **1995**, *501*, C1–C4.

Keywords

Beryllium, Grignard reagents, equilibrium, ligand redistribution, NMR spectroscopy

Table of Contents graphic